UCRL- 86576
PREPRINT

UCRL--86576-5

DESIGNS OF TANDEM-MIRROR FUSION REACTORS

G. A. Carlson, W. L. Barr, B. M. Boghosian,
R. S. Devoto, J. N. Doggett, G. W. Hamilton,
B. M. Johnston, J. D. Lee, B. G. Logan,
R. W. Moir, W. S. Neef,
R. B. Campbell (TRW, Inc.)

This paper was prepared for submittal to
3rd IAEA Workshop on Fusion Reactor Design
and Technology, Tokyo, Japan, October 5-16,
1981.

October 1, 1981

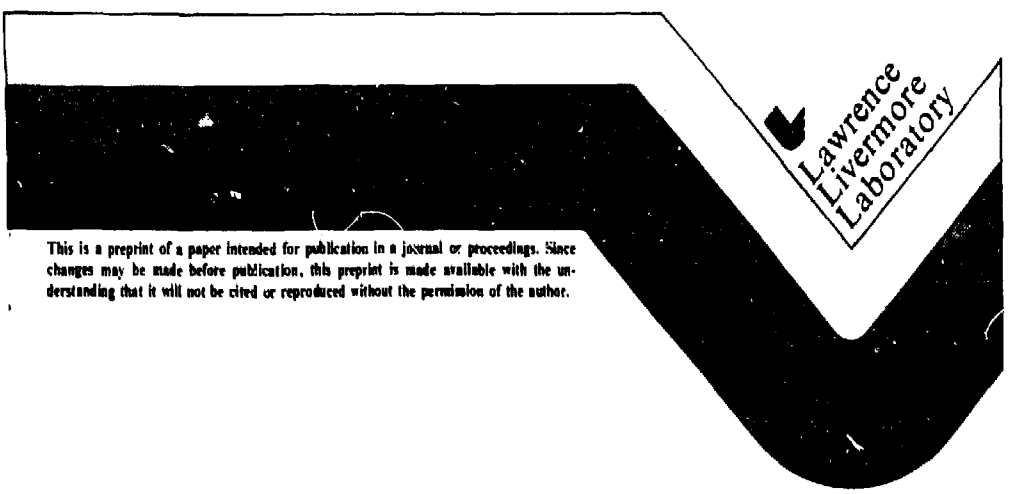

DESIGNS OF TANDEM-MIRROR FUSION REACTORS

G. A. Carlson, W. L. Barr, B. M. Boghosian, R. S. Devoto, J. N. Doggett
G. W. Hamilton, B. M. Johnston, J. D. Lee, B. G. Logan
R. W. Moir, W. S. Neef, R. B. Campbell (TRW, Inc.)

October 1, 1981

Abstract

We have completed a comparative evaluation of several end plug configurations for tandem mirror fusion reactors with thermal barriers. The axi-cell configuration has been selected for further study and will be the basis for a detailed conceptual design study to be carried out over the next two years. The axi-cell end plug has a simple mirror cell produced by two circular coils followed by a transition coil and a yin-yang pair, which provides for MHD stability.

1. INTRODUCTION

To achieve high power density in a tandem mirror fusion reactor (TMR), we must obtain stable confinement of a high-density central cell plasma. The end plugs used in the Tandem Mirror Experiment (TMX) generated the necessary electrostatic fields for central cell plasma confinement by increasing the plug plasma density, but for reactors this strategy is impractical. For TMR's, the confining potential must be enhanced by heating plug electrons which are insulated from those in the central cell by means of a thermal barrier.[1] The thermal barrier is a region of reduced magnetic field, plasma density, and plasma potential between the central cell and the end plug.

During 1981 the effort on magnetic fusion reactor design at LLNL has been devoted to the comparative evaluation of end plug configurations for tandem mirror reactors with thermal barriers. Three different configurations called A-cell, modified-cusp, and axi-cell, have been considered. In each case we have designed the end plug magnets, assessed their physics performance (MHD stability, adiabaticity, etc.), and estimated their cost. We have coupled each end plug with a 150-m-long central cell producing 3500 MW of fusion power at a first wall neutron loading of about 2.3 MW/m^2. We used zero-dimensional fluid models of the tandem mirror plasma to determine the plasma parameters and the end plug power requirements (neutral beams and ECRH). Cost estimates were made for the neutral beams, ECRH, central cell, end-leakage direct converter, reactor building, and balance-of-plant (BOP). A power balance analysis yielded the gross electrical output and the net electrical output for each case. Finally, the cost of power ($/kWe) was calculated for each case by dividing the total direct capital cost by the net electrical output.

In addition to the cost of power, several more subjective figures of merit were considered in our comparative evaluation. These included the concept's degree of dependence on undeveloped technologies and uncertain physics, and the relation of the concept to the ongoing tandem mirror program. All of these considerations led us to select one of the end plug configurations, the axi-cell, for further study.

This paper summarizes our comparative evaluation of the various end plug configurations. Over the next two years LLNL, the University of Wisconsin, and an industrial participant (yet to be chosen) will carry out a detailed conceptual design study of a tandem mirror fusion reactor with axi-cell end plugs.

2. DESIGN OF THE END PLUGS

The three end plug configurations which we considered are the A-cell, the modified-cusp, and the axi-cell. The A-cell configuration is the basis for the MFTF-B design and also the preliminary conceptual design of the Tandem Mirror Next Step facility.[2] The second configuration, the modified-cusp, uses all circular coils, with the fields in some of them opposing the central cell magnetic field. The third configuration, the axi-cell, has a simple mirror cell produced by two circular coils followed by a transition coil and a yin-yang pair.

The magnetic design for the three configurations was carried out with the aid of the magnet design code EFFI and the MHD interchange stability codes STAB and BALLOON. The primary criteria which were considered in the designs were the axial variation of magnetic field strength, MHD interchange stability, adiabaticity for the highest energy confined ions, and, for the non-axisymmetric designs, elimination of the parallel current. Subsidiary criteria included the physical size of the magrets consistent with adequate space for the plasma column and neutron shielding, conductor bundle current density and maximum magnetic field strengths consistent with superconductor technology, and access for neutral beam and rf injection.

Earlier reports have discussed MHD ballooning stability as a more severe constraint than interchange.[3,4] However, subsequent study has indicated that finite-Larmor-radius (FLR) effects in tandem mirrors will greatly ameliorate the effects of ballooning. Here we assume that the actual stability limit will be very close to the interchange stability boundary.

The parallel current issue for the two non-axisymmetric configurations is also evaluated using the STAB code. In general, axial currents are induced in plasmas confined in quadrupole magnetic fields. In a tandem configuration the

magnetic design must be such that no net axial components of diamagnetic plasma current flow from mirror region to mirror region, otherwise magnetic drift surfaces could be grossly distorted. The parallel current between regions is eliminated by designing an axial asymmetry into the yin-yang pair.

2.1 A-cell configuration

Figure 1 shows the end plug magnets (conductor bundles only, excluding coil cases and external structure) for the A-cell configuration. The central cell is to the left of the plug coils. The plug coil arrangement consists of a transition coil, a yin-yang pair, and a C-shaped coil oriented the same as the outer coil of the yin-yang pair. This configuration creates two mirror cells, one in the yin-yang and one between the yin-yang and the C-coil. Both the thermal barrier and the final potential peak are created in the auxiliary mirror cell (the A-cell), whereas mirror-confined ions in the yin-yang cell serve mainly to provide MHD stability.

The on-axis magnetic field strengths at the cardinal points are:

Central cell field, B_c = 3.4 T

Inner and outer yin-yang mirror fields, B_m = 9 T

Yin-yang midplane field, B_0 = 6 T

Minimum field in the A-cell, B_b = 2.3 T

A-cell mirror field $B_{m,a}$ = 9 T

The 9 T mirror fields were chosen because of the expectation that 12 T is a reasonable upper limit for conductor field strengths in yin-yang shaped magnets and that magnet efficiencies ($B_{axis}/B_{conductor}$) greater than 0.75 are difficult to obtain with such a geometry. The 6-T yin-yang midplane field (vacuum mirror ratio of only 1.5) was chosen to favor a high density plasma (good for MHD since the yin-yang has favorable magnetic curvature) rather than

mirror confinement (for which higher mirror ratio would be better). The central cell field strength was chosen to yield the desired fusion power density, and the minimum field in the A-cell evolved from the combined requirements of MHD stability and adiabaticity.

The MHD stability analysis for this design with an assumed A-cell to yin-yang β ratio of 0.9 yielded a maximum allowable central cell to yin-yang β ratio of 1.0. However, we did not eliminate the parallel current in this design; in anticipation of the penalty of doing so we have reduced our design β_c by 20%. We have taken the yin-yang β to be 0.7; thus β_c is 0.56. (All the β values referred to in this paper are peak perpendicular values.)

The A-cell plug magnet set is exactly that developed for the preliminary design of the tandem mirror next step (TMNS).[2] The magnetic forces on each coil are supported by a welded case and a liquid helium-cooled external structure. The major lobe-spreading force on each coil is carried by a box-beam and tensile member structure, as described in Ref. 2. We have assumed the same case and structure masses as for TMNS. The neutron shielding mass estimate for each coil was based on a nominal shield thickness of 0.5 m of steel.

2.2 Modified-cusp configuration

Figures 2 and 3 show the end plug magnets for the modified-cusp configuration. (This present configuration is modified from the originally proposed cusp configuration,[5] which was found to be unacceptable due to poor alpha particle confinement.[6]) The plug coil arrangement consists of a high field solenoid followed by a concentric pair of solenoids. The current of the inner concentric coil opposes the current of all the other coils and produces

a field null on the axis of the machine. A hollow plasma forms because of nonadiabatic losses near the axis. The magnetic flux bundle from the central cell passes as an annulus between the concentric solenoids. This configuration produces only one mirror cell, between the high field solenoid and the concentric pair of solenoids. Both the thermal barrier and the final potential peak are created in this mirror cell. MHD stability is obtained by a combination of favorable magnetic curvature and (for the inner radial region) hot electron stabilization or plasma rotation due to the radial electric field.

The magnetic field strengths at the cardinal points are:

Central cell field, B_c = 3.5 T

Solenoid mirror field, B_{m1} = 20 T

Annulus minimum field, B_b = 2.5 T

Annulus mirror field, B_{m2} = 9 T

The 20 T inner mirror field is created by a compact radially-zoned solenoidal coil composed of normal copper (inner zone) and superconducting Nb_3Sn and NbTi (outer zones). The maximum superconductor field strength is 14 T. The 9 T outer mirror field was chosen so as to limit the maximum conductor field in the concentric solenoids to about 12 T. The central cell field strength was chosen to yield the desired fusion power density, and the minimum field in the annulus evolved from the combined requirements of MHD stability and adiabaticity.

The concentric solenoids have been modeled in EFFI as six separate solenoids, each with a rectangular cross section (see Fig. 3). In actuality, the sides of the coils facing the annular plasma will be contoured to parallel the plasma, thus increasing the space for neutron shielding. This contouring is not expected to affect the magnetics.

The MHD stability analysis for the radially outer flux surface in this design yielded a maximum allowable central cell to barrier β ratio of 2.4. We have taken the central cell β to be 0.7 with a barrier β of 0.6. The inner region of the annular plasma is stabilized by either an induced EXB rotation frequency of 5×10^4 sec^{-1} or by two 50%-beta EBT-type hot electron rings consuming about 14 MW of 120 GHz ECRH.

The location of the inner surface of the hollow, annular plasma is determined by the innermost field line on which the sloshing ions are adiabatically confined in the end cells. The sloshing D+ ions are injected with about 300 keV of energy, and are then accelerated to about 650 keV by the difference in potential before passing through the field minimum in the end cell. We consider the ions to be adiabatically confined if their lifetime is not determined by the scattering in angle due to non-adiabatic jumps in their magnetic moments. For the present design we find that the inner radius of the central cell plasma is about 0.5 m.

All of the coils for the modified-cusp configuration are simple solenoids. The structural design philosophy for the superconducting solenoids is based on using superconductor backed by stainless steel, either bonded or separately wound. The high average stress in the copper insert coil of the 20 T multilayer solenoid necessitates the use of a high strength copper alloy. The annular slot between the concentric solenoids has limited neutron shielding space (~0.25 m) and we use tungsten shielding material there. The copper insert coil must operate unshielded and uses neutron damage resistant MgO conductor insulation.

2.3 Axi-cell configuration

Figure 4 shows the axi-cell end plug magnets. The plug coil arrangement

consists of an axially-spaced pair of solenoids (the first stronger than the second) followed by a transition coil and a yin-yang pair. (In the present design as shown in Fig. 4, we have included a third solenoid, midway between the main two, with its current opposite the other coils' currents. This bucking solenoid serves to shorten the axi-cell, which advantageously reduces the plasma volume there.) This configuration creates two mirror cells, one between the solenoids and one in the yin-yang. The thermal barrier and the final potential peak are created in the axisymmetric cell while the outboard yin-yang (called the anchor) provides a region of favorable curvature for MHD stability. (As a fourth case, we consider a variant of this configuration which eliminates the transition coil and yin-yang pair and provides MHD stability by means of an EBT-type electron ring in the axi-cell.)

The on-axis magnetic field strengths at the cardinal points are:

Central cell field, B_c = 3 T

First axi-cell mirror field, B_{m1} = 20 T

Axi-cell minimum field, B_b = 2.3 T

Second axi-cell mirror field, B_{m2} = 9 T

Inner and outer yin-yang mirror fields, B_m = 4 T

Yin-yang midplane field, B_0 = 2 T

The 20 T mirror field is generated by the same radially-zoned solenoidal coil discussed in the previous section. The 9 T mirror field for the second axi-cell mirror coil was chosen to allow an all-superconducting design with a maximum conductor field strength of 12 T. The yin-yang field strengths were chosen to allow a conservative design (coil efficiency $\approx$50%) with a maximum conductor field strength of only 8 T (permitting the use of MFTF-type NbTi superconductor). The central cell field strength was chosen to yield the desired fusion power density, and the minimum field in the axi-cell evolved

from the combined requirements of MHD stability and adiabaticity.

The MHD stability analysis for this design with equal β's in the central cell and barrier yielded a maximum allowable central cell to yin-yang β ratio of 2.3 for a case with zero parallel current. We have taken the yin-yang β to be 0.3 and the central cell and barrier β's to be 0.7. (For the electron ring stabilized variant of this case we estimate a lower barrier β of 0.55.)

The external structural support for the transition and yin-yang magnets of the axi-cell configuration are box-beam and tensile member structures, similar to those for the A-cell configuration. The solenoid hoop forces are supported by the coil cases and stainless steel bands inside the conductor bundles. Provision is made for 0.5 m of steel neutron shielding on all of the axi-cell magnets except the copper insert coil which must operate unshielded.

3. PLASMA PERFORMANCE

Zero-dimensional and one-dimensional fluid codes have been developed to provide a macroscopic description of the plasma in tandem mirror fusion reactors with thermal barriers. Simply stated, the objective of our plasma model development is to provide a self-consistent set of equations, supported by physics theory and experiment, which can be used to calculate all of the plasma dimensions, densities, energies, potentials, and confinement times in a tandem mirror reactor. The models we developed utilize results from other special purpose plasma codes in a number of ways: Fokker-Planck code results provide guidance for deriving various terms in particle balance equations, MHD codes provide guidance for stability limits on β values, etc. In order to be useful for parametric calculations, our plasma models are programmed for rapid solution by computer.

A series of plasma models has been developed at LLNL to predict the plasma performance for tandem mirrors with thermal barriers. The second generation of this series, consisting of scaling laws for each input power requirement based on the MFTF-B design point, was used to calculate the results given here.

Table I gives the plasma parameters for the four end plug configurations. The magnetic field strengths for these cases have been given previously. The injected power requirements for these cases are given in the next section. In addition to the four primary cases we have also considered the improvement which would result if an alternative barrier pumping scheme, requiring negligible input power, could replace charge exchange pumping. One such possibility is gradient-B drift pumping. To consider such cases we have simply eliminated the charge exchange pump beams in the power balance and the cost estimate. We have assumed that all the plasma parameters of Table 1 (except Q) would remain the same.

4. POWER BALANCE

Figure 5 shows the power flow diagram that we have used to analyze all of the TMR configurations. In all cases we have set the central cell fusion power to 3500 MW. The plasma performance analysis yields the values for injected power trapped in the plug plasmas. In general, these injected powers consist of ECRH and neutral beams (beams for charge exchange pumping of the barrier region, beams for maintaining the sloshing ion distribution in the barrier region, and beams for maintaining the plasma in the MHD anchor). The fusion power divided by the sum of the trapped injected powers is the plasma figure of merit, Q. Associated with each injected power is a trapping fraction, f_i, and an efficiency of production, η_i (see Fig. 5 for the

subscripts used for the various injected powers). The injected powers incident on the plasma are calculated by dividing the trapped injected powers by the f_i's. The electrical input powers to the injectors are calculated by dividing the incident injected powers by the η_i's. Provision is also made for the electrical input power requirements of auxiliary systems. (In the present study, the only auxiliary power we have included is that for operating the normal copper coils.) The sum of all the electrical input powers is the reactor recirculated power.

For DT fusion, 80% of the fusion power is in the form of energetic neutrons. This power is multiplied by the blanket energy multiplication factor M and is made available as heat to the thermal conversion system. There it is converted to electricity at the thermal conversion efficiency, η_T. We estimate the end leakage charged particle power as 20% of the fusion power (the alpha particles) plus the sum of the trapped injected powers. This power is converted to electricity at the electrostatic direct conversion efficiency, η_{DC}. (We have not included a thermal bottoming cycle for the charged particle power.) The sum of the electrical power outputs from the thermal converter and the direct converter is the gross electrical output of the reactor. The gross electrical output minus the recirculated power is the net electrical output of the reactor.

We have used nominal values for the blanket energy multiplication factor and the efficiencies of the beams, ECRH, thermal converter, and direct converter, namely:

$$M = 1.2$$

$$\eta_P = \eta_S = \eta_A = \eta_E = \eta_{DC} = 0.5$$

and $\eta_T = 0.35$

The trapping fractions for the injected powers vary from case to case and have

been calculated as part of the plasma performance analysis.

Table II gives the results of the power balance analysis for the four primary cases, both with and without charge exchange pumping. Recall that for the cases without charge exchange pumping we have simply assumed that the alternative barrier pumping method (e.g., gradient-B drift pumping) would consume negligible power. The modified-cusp cases do not include the 14 MW of trapped ECRH power that might be necessary for hot electron-ring stabilization of the inner region of the annular plasma. For the axi-cell with EBT stabilization, we have included an estimated 56 MW of trapped ECRH power for the hot electron ring.

5. COST ESTIMATE

The methodologies used to estimate the direct capital costs of the various reactor systems are discussed in Ref. 7. For each case these costs, in 1981 dollars, have been divided by the net electrical power to yield a cost of power in $/kwe. The results are summarized in Table III.

6. CONCLUSIONS

The cost of power estimates presented in the previous section show the A-cell configuration to be inferior to either the modified-cusp or the axi-cell. A choice between the modified-cusp and the axi-cell cannot be made solely on the basis of predicted cost of power. Here we chose the axi-cell configuration because MHD stability by means of quadrupole coils has a large and favorable experimental data base. For the axi-cell configuration itself we can tentatively choose the anchor-stabilized case over the EBT-stabilized case on economic grounds. Presently understood theoretical beta limits for the EBT-stabilized case results in a higher cost of power due to lower Q, in

spite of elimination of the anchor mangets. This choice will be re-evaluated as EBT theory and experiments provide new information on beta limits with hot electron rings. The cost of power table clearly shows the advantage of a barrier pumping scheme that consumes less power than charge exchange pumping. At this time, however, the physics of alternative pumping schemes is still uncertain.

REFERENCES

[1] BALDWIN, D.E., LOGAN, B.G., FOWLER, T.K., "An Improved Tandem Mirror Reactor," Lawrence Livermore National Laboratory, Livermore, CA, UCID-18156 (1979).

[2] DAMM, C.C., et al., "Preliminary Design of a Tandem Mirror Next Step Facility," Lawrence Livermore National Laboratory, Livermore, CA, UCRL-53060 (1980).

[3] "Physics Basis for MFTF-B," (BALDWIN, D.E., LOGAN, B.G., SIMONEN, T.C., Eds), Lawrence Livermore National Laboratory, Livermore, CA, UCID-18496, Parts 1 and 2 (1980).

[4] CARLSON, G.A., NEEF, W.S., "Tandem Mirror Reactor Studies at Lawrence Livermore National Laboratory," Lawrence Livermore National Laboratory, Livermore, CA, UCID-18989 (1981).

[5] LOGAN, B.G., "An Axisymmetric, High Beta Tandem Mirror Reactor," Lawrence Livermore National Laboratory, Livermore, CA, UCRL-83555 (1979).

[6] CARLSON, G.A., BARR, W.L., "The Effect of Non-Adiabaticity of Alpha Particles in the Axisymmetric Cusp TMR," Lawrence Livermore National Laboratory, Livermore, CA, UCID-19150 (1981).

[7] CARLSON, G.A., et al., "Comparative End Plug Study for Tandem Mirror Reactors," Lawrence Livermore National Laboratory, Livermore, CA, in preparation.

TABLE I. Plasma parameters

	A-Cell	Modified-Cusp	Axi-cell	Axi-cell with EBT Stabilization
P_{FUSION}	3500 MW	3500	3500	3500
Q	10.3	19.7	22.3	12.2
	(18.2)[a]	(43.8)[a]	(54.7)[a]	(18.5)[a]
Γ_{fw}	2.3 MW/m^2	2.3	2.3	2.2
Central Cell				
r_c	1.1 m	1.0	1.0	1.0
$r_{c,inner}$	--	0.5 m	--	--
r_{fw}	1.3 m	1.3	1.3	1.3
L_c	150 m	150	150	150
β_c	0.56	0.7	0.7	0.7
n_{ic}	1.6×10^{14}cm^{-3}	2.2×10^{14}	1.6×10^{14}	1.6×10^{14}
T_{ic}	40 keV	40	40	40
T_{ec}	36 keV	33	32	33
ϕ_e	270 keV	260	240	240
Barrier				
L_B	8 m	7	8.6	8.6
β_B	0.63	0.61	0.71	0.36
n_{pass}	5.0×10^{12}cm^{-3}	5.5×10^{12}	3.4×10^{12}	4.4×10^{12}
$E_{inj,B}$	350 keV	300	250	250
E_{eh}	520 keV	390	750	240
T_{ew}	93 keV	110	82	150
ϕ_B	230 keV	190	210	170
ϕ_c	150 keV	150	140	140
Anchor				
r_A	0.84 m		1.2	
β_A	0.7		0.3	
n_{iA}	1.7×10^{14}cm^{-3}		1.5×10^{13}	
$E_{inj,A}$	200 keV		150	
E_{iA}	310 keV		150	
T_{eA}	--		32 keV	
ϕ_A	--		160 keV	
ϕ_{pc}	19 keV		--	

[a] Q with no charge exchange pump beams.

TABLE II. Results of Power Balance Analysis
(all powers in MW)

	A-Cell		Modified-Cusp		Axicell		Axi-cell with EBT Stabilization	
Charge exchange pumping	Yes	No	Yes	No	Yes	No	Yes	No
Trapped powers								
ECRH	97	97	60	60	47	47	154	154
Pump beams	148	--	98	--	93	--	97	--
Sloshing beams	66	66	20	20	12	12	35	35
Anchor beams	29	29	--	--	5	5	--	--
TOTAL	340	192	178	80	157	64	286	189
Injected powers								
ECRH	108	108	67	67	52	52	171	171
Pump beams	177	--	118	--	115	--	105	--
Sloshing beams	122	122	83	83	52	52	159	159
Anchor beams	30	30	--	--	15	15	--	--
TOTAL	437	260	268	150	234	119	435	330
Recirculated powers								
ECRH	216	216	134	134	104	104	342	342
Pump beams	354	--	236	--	230	--	210	--
Sloshing beams	244	244	166	166	104	104	318	318
Anchor beams	60	60	--	--	30	30	--	--
Copper coils	--	--	72	72	72	72	72	72
TOTAL	874	520	608	372	540	310	942	732
Thermal converter output	1176	1176	1176	1176	1176	1176	1176	1176
Direct converter output	520	446	439	390	429	382	493	445
TOTAL	1696	1622	1615	1566	1605	1558	1669	1621
Net electrical power	822	1102	1007	1194	1065	1248	727	889

TABLE III. Direct capital costs in $/kWe

	A-Cell		Modified-Cusp		Axi-cell		Axi-cell with EBT Stabilization	
Charge exchange pumping	Yes	No	Yes	No	Yes	No	Yes	No
Beams @$2/W injected	800	278	399	139	342	111	639	352
ECRH @$5/W injected	657	490	333	280	244	208	1176	962
Plug magnets	764	670	249	210	284	242	212	177
Dir. converter	192	143	82	70	143	122	152	128
Central cell	547	408	447	377	423	361	545	455
Reactor bldg.	201	150	153	129	152	130	180	151
BOP	572	426	467	394	441	377	569	476
TOTAL	3733	2465	2130	1599	2029	1551	3473	2701

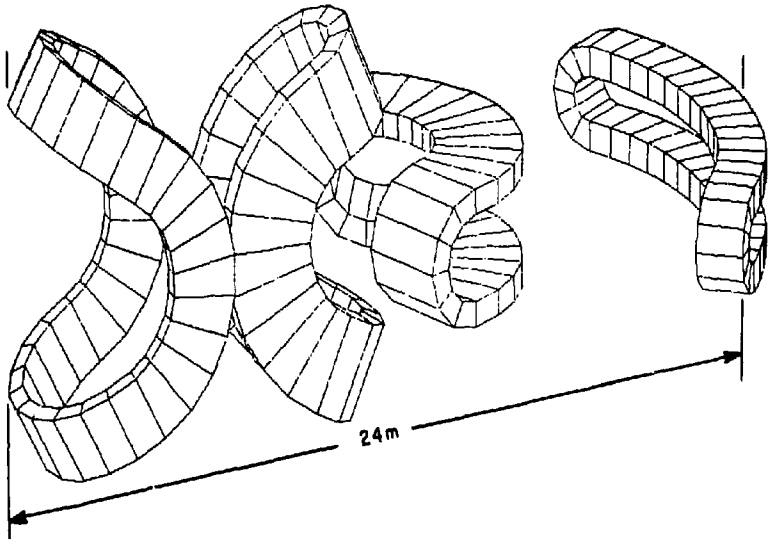

74-101-0

FIG. 1 End plug magnets for A-cell TMR.

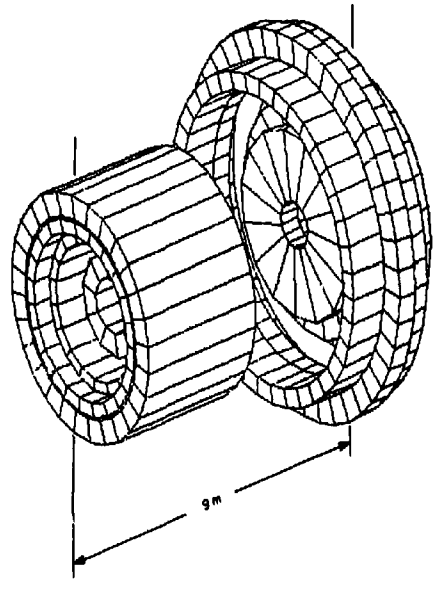

74-102-01

FIG. 2 End plug magnets for modified-cusp TMR.

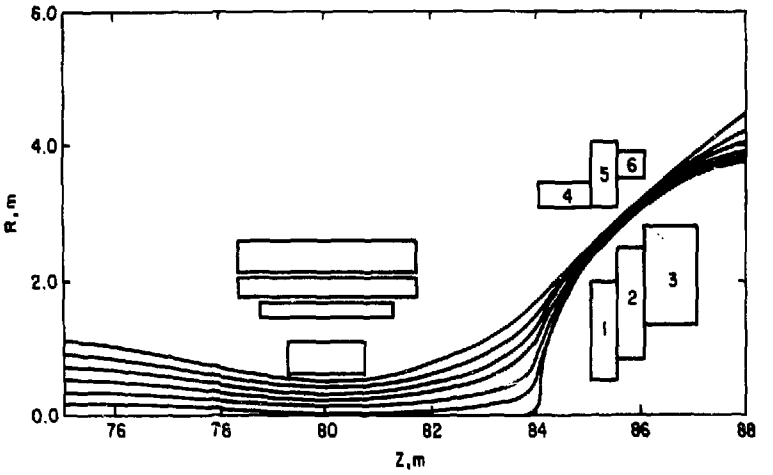

FIG. 3 Cross section of end plug magnets for modified-cusp TMR.

74-102-013

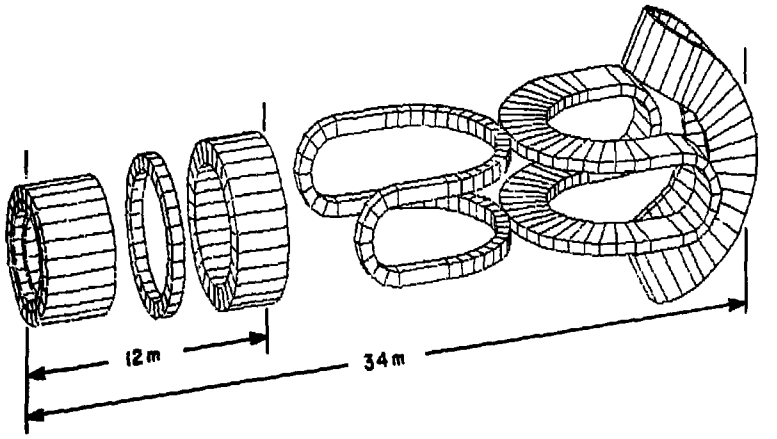

74-102-011

FIG. 4 End plug magnets for axi-cell TMR.

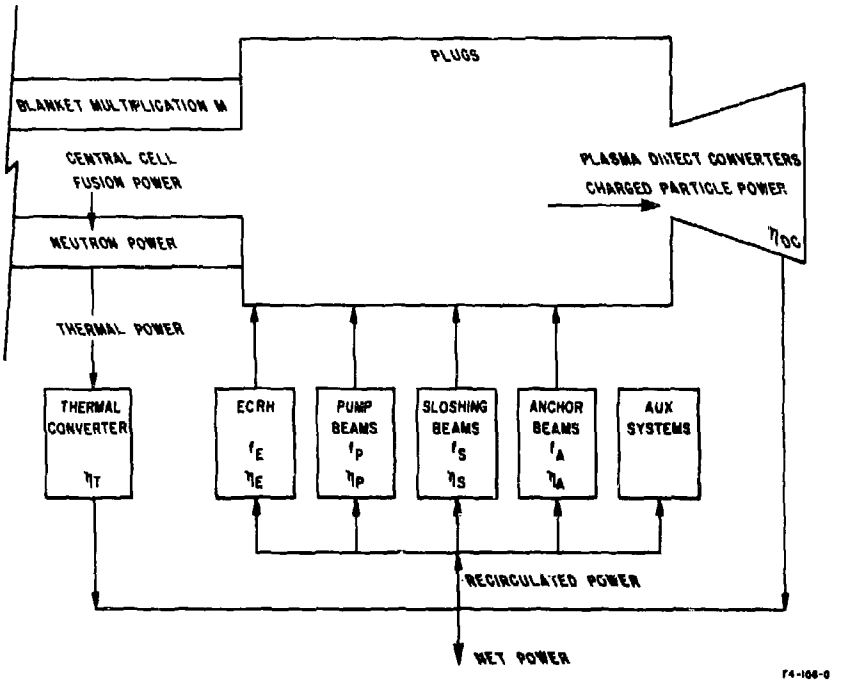

FIG. 5 Power flow diagram.